S1 The Radar Equation

This section describes how to derive the absolute reflectivity calibration constant of a Frecuency Modulated Continuous Wave (FMCW) radar. This procedure can also be applied for pulsed doppler radars by using their corresponding radar equation.

The radar equation describes the physical power budget of a signal emitted by the radar from the moment it enters the transmitter antenna until it is received by the receiver antenna. At the beginning, the transmitted signal is generated by the radar emitter chain. This signal enters the emitter antenna with a power P'_t (physical power, for example in milliwatt units). Usually radar antennas are very directive, with one main lobe oriented in the direction of observation. The maximum gain of the transmitter antenna lobe is defined as G_t.

Figure S1 shows the geometrical configuration of a system with a radar and an scattering object placed at a distance r. Assuming the radar transmitter antenna is aligned in the angle of maximum gain with this target, the object will receive a power density $P_{rec}(\vec{r})$ of:

$$P_{rec}(\vec{r}) = P'_t \frac{G_t}{4\pi r^2} \tag{S1}$$

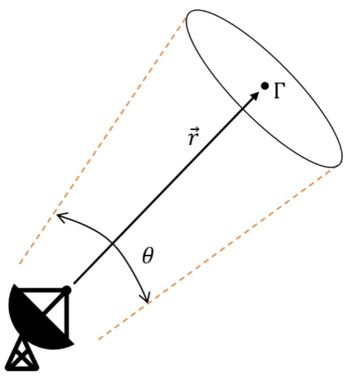

Figure S1: Radar pointing towards a target with cross section Γ, located at a distance r. θ is the beam width of the antennas.

The Radar Cross Section (RCS) Γ of an object can be understood as the equivalent cross-sectional area a sphere should have to reflect the same amount of incident power back to the radar receiver. The units to represent RCS are m^2 in physical scale, and $dBsm$ in dB scale ($dBsm = 10 \log_1 0(\Gamma(m^2)))$. The the density of power backscattered by this object, at its position $\vec{r}$, is:

$$P_{refl}(\vec{r}) = P'_t \frac{G_t}{4\pi r^2} \Gamma \tag{S2}$$

The radar used in this experiment has two parallel antennas with a distance between each other comparable to their diameter. If the reflecting object is at a distance several orders of magnitude larger than the antenna separation, it is possible to assume that the instrument is operating in full antenna overlap conditions. This means that both antennas share the same field of view at that location. With this assumption and considering the power spread caused by a wave traveling back to the radar a distance r and the receiver antenna aperture $A_p = G_r \lambda^2 / 4\pi$, we have a physical power being output at the receiver antenna end of P'_r.

$$P'_r = \frac{G_t P'_t}{4\pi r^2} \frac{A_p}{4\pi r^2} \Gamma = \frac{G_t G_r \lambda^2 P'_t}{(4\pi)^3 r^4} \Gamma \tag{S3}$$

Equation (S3) is known as the General Radar Equation. From this equation it is theoretically possible to retrieve the Γ value of a target from P_r' measurements, provided a way to measure its distance r (for example FMCW radars use signals with varying frequency to measure the distance to the target [Delanoë et al., 2016]).

Radar operators work with power variables defined by the pair $P_t' = L_t P_t$ and $P_r' = L_r P_r$. Here L_t and L_r represent all the gains and losses introduced by hardware elements, which determine the actual physical power emitted. P_t and P_r are emitted and received power values output by the radar in arbitrary units, proportional to the physical values. The calibration need appears here, because radar gains and losses are difficult to quantify, and without knowing their values it is impossible to retrieve the physical power budget. Antenna gain and radome attenuation also plays a role, increasing the amount of characterizations needed [Anagnostou et al., 2001].

So far we have neglected in the calibration equation the impact of atmospheric attenuation L_{at}. Attenuation is introduced by the presence of gases, which absorb power from the propagating wave. This attenuation can be significant for W band radars. For example at our site it can be reach values of $\approx 0.8\ dB\ km^-1$ in the horizontal, depending on absolute humidity and pressure conditions. Including attenuation, Eq. (S3) becomes:

$$P_r = \frac{L_r G_t G_r \lambda^2 P_t}{L_t (4\pi)^3} \frac{\Gamma}{L_{at}^2 r^4} \tag{S4}$$

We begin by defining the constant terms as the RCS calibration term C_Γ (Eq. (S5)). We observe that this term enables the calculation of an observed RCS Γ from P_r and r measurements, by using the Radar Equation (Eq. (S6)). Atmospheric attenuation can be estimated from measurements of atmospheric properties and the use of microwave propagation models such as the one proposed by Liebe [1989].

$$C_\Gamma = \frac{L_t (4\pi)^3}{L_r G_t G_r \lambda^2 P_t} \tag{S5}$$

$$\Gamma = C_\Gamma\ L_{at}^2 r^4 P_r \tag{S6}$$

As seen by its definition, the calculation of C_Γ requires the knowledge of the complete power budget in transmitter and receiver including antenna gain. This is usually difficult to measure accurately due to the amount of components and interactions to be tested. However, other methods exist. From Eq. (S6) it is possible to infer that by placing a discrete object with known cross section $\Gamma = \Gamma_0$ at a known distance r_0, and with monitored atmospheric conditions, we become able to retrieve *externally* the calibration constant C_Γ (Eq. (S7)) by sampling the power $P_r(r_0)$ reflected back. This procedure is known as end-to-end calibration because it characterizes the complete system at once.

$$C_\Gamma = \frac{\Gamma_0}{L_{at}^2 r_0^4 P_r(r_0)} \tag{S7}$$

Obtaining C_Γ is usually enough for many radar applications, since it enables the estimation of the RCS of an object. Nevertheless, for meteorological radars the main interest is in retrieving the Equivalent Reflectivity Z_e of a volume filled with small scatterers (water droplets or ice crystals). Equivalent reflectivity has the advantage that it enables the comparison between measurements of different wavelength radars.

FMCW radars have a distance resolution δr which depends on its chirp configuration. These points of differentiated resolution are called *gates*. When the instrument operates using antennas with beam width θ (in radians) and a Gaussian Beam Pattern, each gate will have the effective sampling volume V indicated in Eq. (S8).

$$V = \frac{\pi \delta r}{2 \ln 2} \left(\frac{r\theta}{2} \right)^2 \tag{S8}$$

Assuming that target particles are spheres with a diameter D and a size distribution per unit volume of $N(D)$, and that most of them have a size factor in the Rayleigh Scattering regime Wallace and Hobbs [2006], the total cross section of a volume filled with them can be estimated as:

$$\sigma_v = \frac{\pi^5 K^2}{\lambda^4} V \int_0^\infty N(D) D^6 dD \tag{S9}$$

Where $K^2 = (\epsilon - 1)^2/(\epsilon + 2)^2$ is a constant with a value which depends on the complex electrical permittivity ϵ of the scatterers. From here arises a microphysical definition of Z_e, in units of $mm^6 m^{-3}$ (Eq. (S10)).

$$Z = 10^{18} \int_0^\infty N(D) D^6 dD \tag{S10}$$

Replacing Eqs. (S8), (S9) and (S10) into eq. (S4), one obtains the relationship between Received power and Reflectivity (Eq. (S11)).

$$Z = \frac{512 \ln(2) \lambda^2 L_t 10^{18}}{G_t G_r \theta^2 \pi^3 K^2 L_r P_t \delta r} L_{at}^2 r^2 P_r \tag{S11}$$

From Eq. (S11) we can define a calibration constant for reflectivity: C_Z. If the value of K^2 chosen corresponds to that of liquid water ($|K| \approx 0.86$ at 95 GHz and $5°C$[Meissner and Wentz, 2004]) it is possible to retrieve the microphysical Equivalent Reflectivity of suspended water droplets in fog or clouds!

$$Z = C_Z \; L_{at}^2 r^2 P_r \tag{S12}$$

As a final remark, we can use Eq. (S13) to link C_Γ with C_Z. This procedure is easier to do when compared to the internal calibration, and therefore we propose to calibrate the radar by first retrieving C_Γ from an end-to-end calibration approach, and then use this result to calculate C_Z.

$$C_Z = \frac{8 \ln(2) \lambda^4 10^{18}}{\theta^2 \pi^6 K^2 \delta r} C_\Gamma \tag{S13}$$

S2 Geometrical RCS simulator

This simulator enables the calculation of the perceived RCS for a given geometric configuration of the system. At this point it works only for trihedral reflectors. For the radar's antenna pattern it is possible to use a Gaussian model, or to input a beam shape manually. In this document we'll only show the gaussian function, since adapting the equations to consider other shapes is straightforward.

The input arguments for the RCS simulator are shown in Fig. S2 (Left). They are explained as follows:

- Radar position, referenced at the origin O: $\vec{R_O} = (x_r, 0, h_r)$
- Radar aiming angle, referenced at the origin O_r: $\vec{Y_{O_r}} = (1, \theta_r, \phi_r)$
  - θ_r: Azimuth angle of the radar's positioner. 0° is vertical aiming.

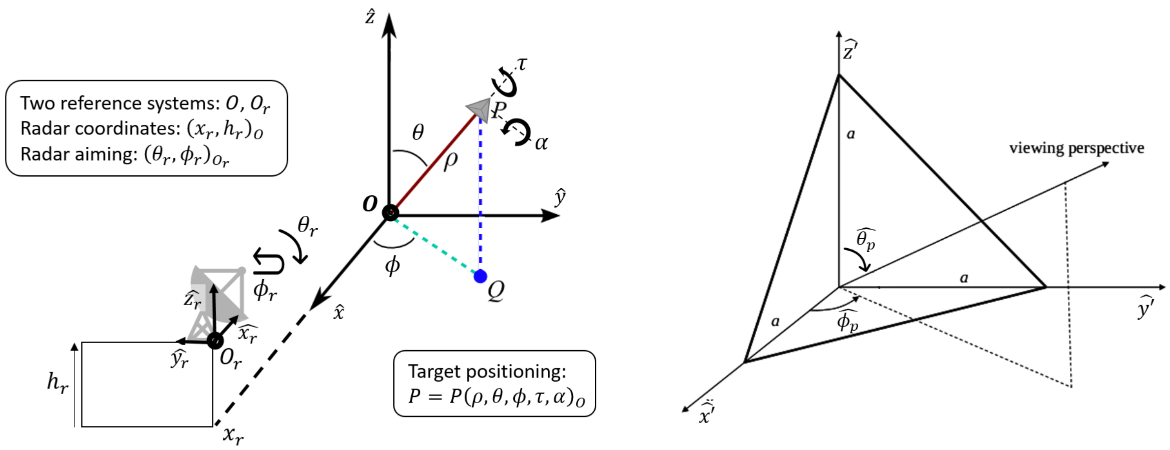

Figure S2: Diagram of the geometrical RCS simulator. (Left) shows the coordinate axes and the degrees of freedom of the simulator. (Right) shows the coordinates used to characterize the beam's incidence angle on the target. Right figure is adapted from the one published by Doerry and Brock [2009].

  - ϕ_r: Azimuth angle of the positioner. The line connecting the radar and the mast base corresponds to $\phi_r = 0°$.

- Target position (in spherical coordinates), referenced at the origin O: $\vec{T_O} = (\rho, \theta, \phi)$
  - τ: Mast twist angle. $\tau = 0°$ when target boresight is parallel to the x axis.
  - α: Target tilt angle. When $\alpha = 0°$ the target's z' axis is parallel to $\hat{\rho}$. If $\alpha > 0°$ then the target tilts forward.
- a: Target's size parameter [Brooker, 2006].
- λ: Wavelength
- Antenna properties (if using Gaussian model):
  - Θ: antenna beamwidth

Output variables:

- Maximum RCS of the target $\Gamma_0[dBm^2]$
- RCS of the target for the beam's incidence vector $\hat{r_i}$: $\Gamma(\vec{r_i})[dBm^2]$
- Effective RCS of the target considering incidence angle and loss L due to positioning $\Delta D°$ away from the antenna's beam center: $\Gamma_{eff} = \Gamma(\vec{r_i}) - 2L(\Delta D)[dB]$

In the following sections we list the equations used to calculate each term.

S2.1 Max theoretical RCS Γ_0

From Brooker [2006], it can be simply calculated as:

$$\Gamma_0[dBm^2] = 10\log_{10}(\frac{4\pi a^4}{3\lambda^2}) \tag{S14}$$

S2.2 RCS $\Gamma(\vec{r_i})$ for the beam's incidence vector

We obtain the perspective vector by changing radar aiming vector's Y_{O_r} coordinate system from O_r to O, and then multiplying by -1 to reverse the resulting vector's direction.

$$\vec{r_i} = -1\left(-(\vec{Y_{O_r}} \cdot \hat{x_r})\hat{x} - (\vec{Y_{O_r}} \cdot \hat{y_r})\hat{y} + (\vec{Y_{O_r}} \cdot \hat{z_r})\hat{z_r}\right) \tag{S15}$$

Target's unitary vectors $\hat{x'}$, $\hat{y'}$, $\hat{z'}$ (in Fig. S2 (A)):

$$\begin{aligned}\hat{x'} = \frac{\sqrt{2}}{2}\big[&-\sin(\theta)\cos(\phi)\sin(\alpha)+\cos(\theta)\cos(\phi)(\cos(\alpha)\cos(\tau)+\sin(\tau))-\sin(\phi)(\cos(\alpha)\sin(\tau)-cos(\tau))\big]\hat{x}\\ &+\big[\sin(\theta)\sin(\phi)\sin(\alpha)+\cos(\theta)\sin(\phi)(\cos(\alpha)\cos(\tau)+\sin(\tau))+\cos(\phi)(\cos(\alpha)\sin(\tau)-\cos(\tau))\big]\hat{y}\\ &+\big[-cos(\theta)sin(\alpha)-sin(\theta)(\cos(\alpha)\cos(\tau)+\sin(\tau))\big]\hat{z}\end{aligned} \tag{S16}$$

$$\begin{aligned}\hat{y'} = \frac{\sqrt{2}}{2}\big[&-\sin(\theta)\cos(\phi)\sin(\alpha)+\cos(\theta)\cos(\phi)(\cos(\alpha)\cos(\tau)-\sin(\tau))-\sin(\phi)(\cos(\alpha)\sin(\tau)+\cos(\tau))\big]\hat{x}\\ &+\big[\sin(\theta)\sin(\phi)\sin(\alpha)+\cos(\theta)\sin(\phi)(\cos(\theta)\cos(\tau)-\sin(\tau))+\cos(\phi)(\cos(\alpha)\sin(\tau)+\cos(\tau))\big]\hat{y}\\ &+\big[-\cos(\theta)\sin(\alpha)-\sin(\theta)(\cos(\alpha)\cos(\tau)-\sin(\tau))\big]\hat{z}\end{aligned} \tag{S17}$$

$$\begin{aligned}\hat{z'} = \big[&\sin(\theta)\cos(\phi)\cos(\alpha)+\cos(\theta)\cos(\phi)\sin(\alpha)\cos(\tau)-\sin(\phi)\sin(\alpha)\sin(\tau)\big]\hat{x}\\ &+\big[\sin(\theta)\sin(\phi)\cos(\alpha)+\cos(\theta)\sin(\phi)\sin(\alpha)\cos(\tau)+\cos(\phi)\sin(\alpha)\sin(\tau)\big]\hat{y}\\ &+\big[\cos(\theta)\cos(\alpha)-\sin(\theta)\sin(\alpha)\cos(\tau)\big]\hat{z}\end{aligned} \tag{S18}$$

Project perspective vector to target's coordinate system:

$$x_p = \vec{r_i} \cdot \hat{x'} \tag{S19}$$
$$y_p = \vec{r_i} \cdot \hat{y'} \tag{S20}$$
$$z_p = \vec{r_i} \cdot \hat{z'} \tag{S21}$$

Then we can calculate the perspective angles θ_p and ϕ_p:

$$p = \sqrt{x_p^2 + y_p^2 + z_p^2} \tag{S22}$$
$$\theta_p = \arccos(z_p/p) \tag{S23}$$
$$\phi_p = \arctan(y_p/x_p) \tag{S24}$$
$$\tag{S25}$$

Invalid cases: If θ_p or $\phi_p \notin [0, \frac{\pi}{2}]$, $\Gamma(\vec{r_i})$ is set to Nan (not a number). This avoids ill results that may happen in configurations where the incident beam is not impacting the interior of the reflector.

Finally, we can use valid θ_p and ϕ_p angles and the equations published by Doerry and Brock [2009] to calculate $\Gamma(\vec{r_i})$:

$$\Gamma(\vec{r_i}) = \begin{cases} \frac{4\pi}{\lambda^2} a^4 \left(\frac{4c_1c_2}{c_1+c_2+c_3}\right)^2 & \text{for } c_1 + c_2 \leq c_3 \\ \frac{4\pi}{\lambda^2} a^4 \left(c_1 + c_2 + c_3 - \frac{2}{c_1+c_2+c_3}\right)^2 & \text{for } c_1 + c_2 > c_3 \end{cases} \tag{S26}$$

For c_1, c_2 and c_3, we assign one of the terms indicated below, imposing $c_1 \leq c_2 \leq c_3$.

$$\left.\begin{matrix} c_1 \\ c_2 \\ c_3 \end{matrix}\right\} = \begin{cases} \cos(\theta_p) \\ \sin(\theta_p)\sin(\phi_p) \\ \sin(\theta_p)\cos(\phi_p) \end{cases} \tag{S27}$$

S2.3 Effective RCS Γ_{eff} considering the incidence vector and beam alignment

Since we already calculated $\Gamma(\vec{r_i})$ in the previous section, we only have left to estimate the losses $L(\Delta D)$ in the effective RCS introduced when the target is ΔD off the center of the beam. This calculation assumes an axially symmetric beam, but can be adjusted to consider beams with other shapes.

First, the vector connecting radar and target position:

$$\vec{\delta_O} = T_O - R_O \tag{S28}$$

We now change the origin of $\vec{\delta_O}$ from O to O_r:

$$\vec{\delta_{O_r}} = -(\vec{\delta_O} \cdot \hat{x})\hat{x_r} - (\vec{\delta_O} \cdot \hat{y})\hat{y_r} + (\vec{\delta_O} \cdot \hat{z})\hat{z_r} \tag{S29}$$

With this vector and the radar's unitary aiming vector Y_{O_r} we can proceed to calculate the angular deviation ΔD of the target from the center of the beam:

$$\Delta\theta = \arccos\left(\frac{\delta_{O_r} \cdot \hat{z_r}}{\|\delta_{O_r}\|}\right) - \theta_r \tag{S30}$$

$$\Delta\phi = \arctan\left(\frac{\delta_{O_r} \cdot \hat{y_r}}{\delta_{O_r} \cdot \hat{x_r}}\right) - \phi_r \tag{S31}$$

$$\Delta D = \sqrt{\Delta\theta^2 + \Delta\phi^2} \tag{S32}$$

$$\tag{S33}$$

And the loss, for the Gaussian antenna lobe of beamwidth Θ, is:

$$L(\Delta D) = 10\log_{10}\left(exp\left(\frac{-(2.355\Delta D)^2}{2\Theta^2}\right)\right)[dB] \tag{S34}$$

Invalid cases: We have observed that four our antenna the Gaussian approximation works well if $\Delta D \leq 0.5°$ (figure 3 of the article). Thus, we decided that any ΔD larger than $0.5°$ our calculations will return an invalid $L(\Delta D)$ value.

With all these terms and Eq. (S35) we finally calculate the effective RCS Γ_{eff}:

$$\Gamma_{eff} = \Gamma(\vec{r_i}) - 2L(\Delta D)[dB] \tag{S35}$$

S3 Misalignment bias in calibration using reference reflectors

Equation (S36) is the Radar Cross Section (RCS) calibration constant, obtained when aiming the radar towards a reference reflector of RCS Γ_0. L_{at} represents the atmospheric attenuation between the radar and the reflector, located at a distance r_0. $P_r(r_0)$ is the power received from the target's position. This equation requires a perfect alignment between the target's boresight and the axis of the antenna lobe.

$$C_\Gamma^0[dB] = \Gamma_0[dBm^2] - 2L_{at}[dB] - 40\log_{10}(r_0) - P_r(r_0) - n(T - T_0) \tag{S36}$$

W band radars tend to have very narrow beam lobes, in the order of 0.5 - 1.0^o. This implies that an error of 1^o in the system's alignment may induce a change of the perceived RCS in the order of some dBs. We define the effective RCS Γ_i as the RCS that will be observed by the radar when the target is off the beam center, or when the target is not in its designed positioning. i.e. the RCS that a perfectly calibrated radar would perceive under a non-ideal alignment.

If we use Eq. (S36) to calibrate assuming RCS $= \Gamma_0$, but in reality we have an effective RCS $\Gamma_i = \Gamma_0 - \epsilon_i$, our estimated calibration constant will be biased:

$$C_{\Gamma i}^0 = C_\Gamma^0 + \epsilon_i \tag{S37}$$

Where $C_{\Gamma i}^0$ and C_Γ^0 are the experimental and the real RCS calibration coefficients after temperature correction, and ϵ_i is the calibration bias. The value of the bias term ϵ_i is difficult to estimate, because it follows an unkown distribution which depends on the alignment uncertainty of all the components in the system. Besides, if the average bias value $\bar{\epsilon} \neq 0$ (i.e. its distribution is not zero mean), this error won't be canceled when averaging $C_{\Gamma i}^0$ values from multiple experiments.

$$\frac{1}{N}\sum_{i=1}^{N} C_{\Gamma i}^0 = \frac{1}{N}\sum_{i=1}^{N}(C_\Gamma^0 + \epsilon_i) = C_\Gamma^0 + \overline{\epsilon_i} \tag{S38}$$

Figure 6 (B) in the main article shows a sample Γ_i distribution obtained when including uncertainty in the experiment's alingment. We can clearly observe that it's not zero mean. This implies that without further correction our calibration constant is bound to have a bias $\overline{\epsilon_i}$, linked to the underlying uncertainty in the positioning of each element.

To estimate the value of $\overline{\epsilon_i}$ for our setup, we use the standard deviation σ between C_Γ^0 values retrieved in each experiment as an indicator of their bias distribution, as indicated in Eq. (S39). σ_ϵ is the standard deviation of the bias distribution.

$$\sigma^2 = \frac{1}{N}\sum_{i=1}^{N}(C_{\Gamma i}^0 - \overline{C_{\Gamma i}^0})^2 = \sigma_\epsilon^2 \tag{S39}$$

By simulating effective RCS values we can relate σ_ϵ with $\overline{\epsilon_i}$ to a given degree of uncertainty. The procedure for doing this is explained in Sect. S3.1.

S3.1 Estimation of the bias term

In this section we explain how we sample the bias distribution, to calculate the bias correction term and its uncertainty. We'll explain the procedure using the results of the 2018 campaign to illustrate (figure 7 of the main article).

The first step we take is to simulate a meta-distribution $f_{\overline{\epsilon_i},\sigma_e psilon}(\overline{\epsilon_i}, \sigma_\epsilon)$. This distribution is generated by calculating the outcome of an experiment with N iterations, with randomly generated uncertainty sets as inputs (see section 5.5 in the main article). From each of these outcomes we get a pair $(\overline{\epsilon_i}, \sigma_e psilon)$, and their distribution will indicate the shape of f.

For the 2018 campaign we sampled the meta-distribution when performing 6 experiments using the following uncertainty set generating functions:

- $\sigma_{\theta_r} = \mathcal{U}([0°, 0.375°])$
- $\sigma_{\phi_r} = \mathcal{U}([0°, 0.375°])$
- $\sigma_{\theta} = \mathcal{U}([0°, 5°])$
- $\sigma_{\tau} = \mathcal{U}([0°, 10°])$

The region where σ_{θ_r} and σ_{ϕ_r} are sampled is within 0 and 3 times the nominal resolution of the radar positioner. For the mast angles θ and τ we have chosen to explore an space much larger than any deviation we have observed during the experiments. We found that with these parameters the sampling covers a range of σ_ϵ values large enough to enable an estimation of the bias in our experiment.

Figure S3 shows the resulting $f_{\overline{\epsilon_i}|\sigma_\epsilon}(\overline{\epsilon_i}, \sigma_\epsilon)$. We can observe that the distribution loses density for relatively large values of $\overline{\epsilon}$ and σ_ϵ. However, the distribution is very well defined around our results of the calibration experiment of 2018, where we got a value of $\sigma_\epsilon = 0.33$.

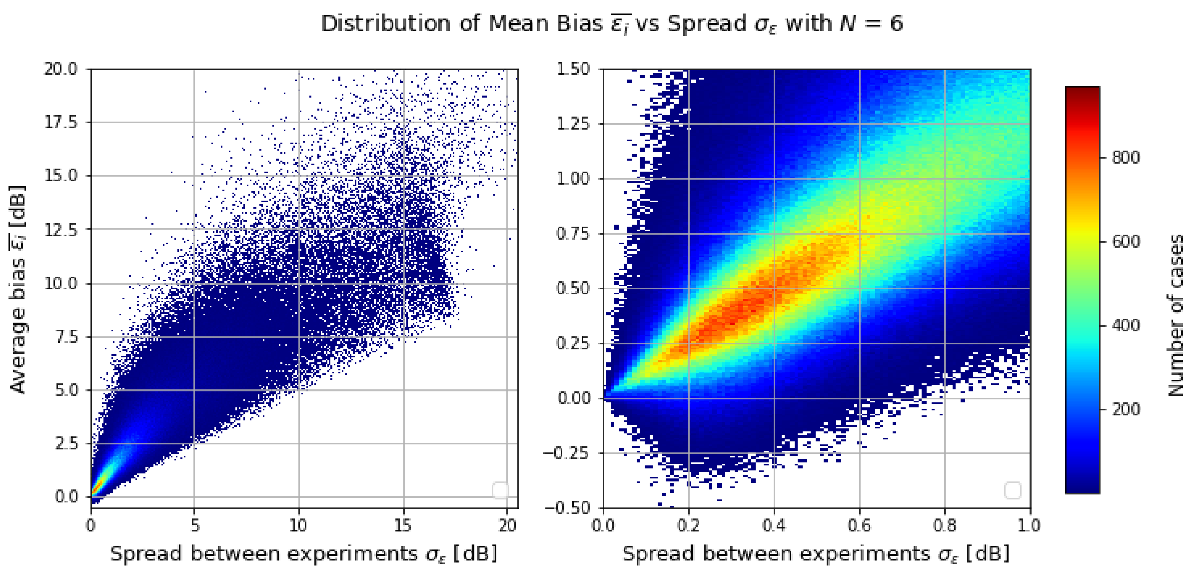

Figure S3: Simulation of $P\left(\sum_{i=1}^{N} \epsilon_i\right)$. This meta-distribution enables the approximation of Λ by selecting the points close to the observed σ_ϵ value. The distribution is very well defined for values of σ_ϵ below one dB, and remains the same even after removing randomly half of the points.

To select the data matching our experiment we define the new distribution $\Lambda = f_{\overline{\epsilon_i}|\sigma_\epsilon=(\sigma\pm5\%)}(\overline{\epsilon_i})$. The resulting distribution is shown in Fig. S4.

Since Λ is asymmetric, we use the median $\tilde{\Lambda}$ as the most likely bias, and its RMSE σ_Λ as its uncertainty contribution. This way we can now correct the bias in the calibration using Eq. (S40).

$$\hat{C_\Gamma^0} = \frac{1}{N}\sum_{i=1}^{N} C_{\Gamma i}^0 - \tilde{\Lambda} \tag{S40}$$

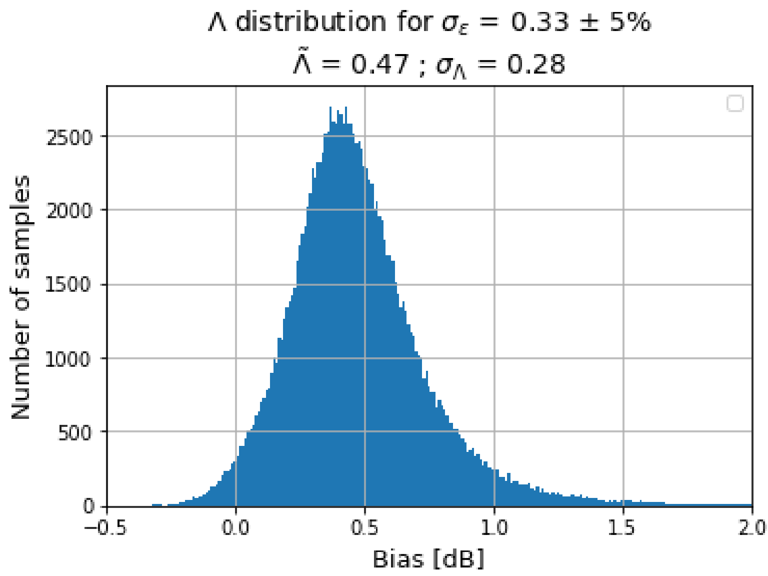

Figure S4: Lambda distribution

S4 Recommendations for future Calibration Experiments

Here we include recommendations that could be valuable for people interested in repeating the article experiment at other sites:

1. The target must be positioned far enough to avoid significant antenna overlap losses, and to avoid receiver saturation. Here a receiver saturation curve is a very valuable asset.
2. Clutter from the target environment must be properly caracterized to determine if target RCS is enough for the level of accuracy desired. Here a determination of the signal to clutter ratio becomes essential. First and second points are key to evaluate if the calibration experiment is viable.
3. Several repetitions of setup realignment and calibration sampling are necessary to estimate mis-alignment bias. To have a valid bias correction both radar and target must be realigned using always the same protocol. This procedure should be clearly stablished and well known by the operating team. Mast alignment in particular can be very demanding both in time and skill.
4. A characterization of radar gain variations for different internal temperatures is necessary to confirm or discard an impact in the calibration stability. This is specially important for radars built with solid state components.
5. Atmospheric conditions must be monitored at the experiment location. We modeled attenuation at different levels based on measurements retrieved with a 20 m tower at the SIRTA observatory, and verified that a single measurement at the surface was representative for our setup. If the target is installed in a taller mast it is advisable to perform this check, to avoid biases from non-representative atmospheric attenuation modeling.
6. The experiment has to be carried out under clear conditions at the surface. No fog or precipitation is tolerable. Also wind speed should remain low ($\leq 1\ ms^{-1}$). We observed that strong wind gusts can perturb the alignment of the system, and, therefore, modify the calibration results, due to the aerodynamic resistance of the mast. We found that the best conditions for calibration at our site usually happen at nighttime under clear sky conditions.
7. The use of an electronic aiming device for the target provides logistical advantages, because there is no more need of physically accesing the mast to perform re-alignments. This drastically reduced the amount of time needed to perform each iterations, from half a day with the 20 m mast setup to approximately 5 minutes with the 10 m mast.

References

J. Delanoë, A. Protat, J-P. Vinson, W. Brett, C. Caudoux, F. Bertrand, J. Parent du Chatelet, R. Hallali, L. Barthes, M. Haeffelin, et al. Basta: a 95-ghz fmcw doppler radar for cloud and fog studies. *Journal of Atmospheric and Oceanic Technology*, 33(5):1023–1038, 2016.

Emmanouil N. Anagnostou, Carlos A. Morales, and Tufa Dinku. The use of trmm precipitation radar observations in determining ground radar calibration biases. *Journal of Atmospheric and Oceanic Technology*, 18(4):616–628, 2001. doi: 10.1175/1520-0426(2001)018<0616:TUOTPR>2.0.CO;2. URL `https://doi.org/10.1175/1520-0426(2001)018<0616:TUOTPR>2.0.CO;2`.

H. J. Liebe. Mpm—an atmospheric millimeter-wave propagation model. *International Journal of Infrared and millimeter waves*, 10(6):631–650, 1989.

J. M. Wallace and P. V. Hobbs. *Atmospheric science: an introductory survey*, volume 92. Elsevier, 2006.

T. Meissner and F. J. Wentz. The complex dielectric constant of pure and sea water from microwave satellite observations. *IEEE Transactions on Geoscience and Remote Sensing*, 42(9):1836–1849, Sep. 2004. ISSN 0196-2892. doi: 10.1109/TGRS.2004.831888.

A. W. Doerry and B. C. Brock. Radar cross section of triangular trihedral reflector with extended bottom plate. *Sandia Report, Sandia National Laboratory*, 2009.

G. Brooker. *Sensors and signals.* Citeseer, Australian Centre for Field Robotics, Rose St Building (J04), University of Sydney, Australia, 2006.